ACS Catalysis

Research Article

pubs.acs.org/acscatalysis

Kinetics of Homogeneous Brønsted Acid Catalyzed Fructose Dehydration and 5-Hydroxymethyl Furfural Rehydration: A Combined Experimental and Computational Study

T. Dallas Swift,[†,§] Christina Bagia,[†,§] Vinit Choudhary,[†,§] George Peklaris,[‡,§] Vladimiros Nikolakis,*[,†,§] and Dionisios G. Vlachos*[,†,§]

[†]Department of Chemical and Biomolecular Engineering, University of Delaware, 150 Academy Street, Newark, Delaware 19716, United States

[‡]Department of Chemical Engineering, University of Massachusetts, 686 North Pleasant Street, 159 Goessmann Lab, Amherst, Massachusetts 01003, United States

[§]Catalysis Center for Energy Innovation, 221 Academy Street, Newark, Delaware 19716, United States

Supporting Information

ABSTRACT: We perform the first extensive experimental kinetic studies of fructose dehydration and 5-hydroxymethyl furfural (HMF) rehydration at low temperatures over a wide range of conditions ($T \sim 70-150$ °C; pH values 0.7−1.6 and initial concentrations of fructose (5−20%w/v) and HMF (2.5−10%w/v)). Guided from insights from our first-principles calculations, we perform kinetic isotope effect (KIE) experiments of labeled fructose to validate the rate-limiting step. Subsequently, we develop the first skeleton model for fructose dehydration and HMF rehydration that integrates the fundamental kinetic experiments and accounts for the KIE, as well as the distribution of fructose tautomers, which changes significantly with temperature, and a direct path of fructose conversion to formic acid. It is shown that the skeleton mechanism of two steps consisting of fast protonation and dehydration followed by intramolecular hydride transfer as the rate-limiting step can capture the experimental kinetics and KIE experiments well. Fructose dehydration is found to result in stoichiometric excess of formic acid relative to levulinic acid, produced directly from fructose. All reactions are shown to be pseudo-first order in both catalyst and substrate. These insights are incorporated in a continuous flow reactor model; higher temperatures improve the optimum yield of HMF, while HMF selectivity at low conversions is less sensitive to temperature.

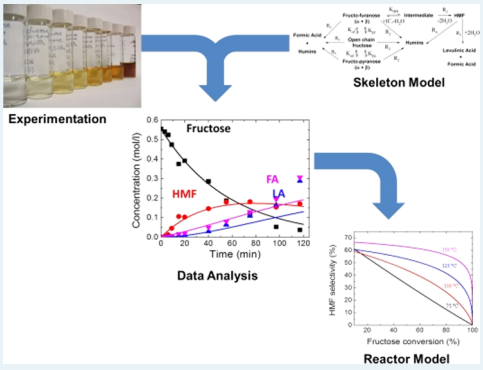

KEYWORDS: *kinetics, dehydration, HMF, fructose, tautomerization, modeling, intrahydride transfer*

INTRODUCTION

Furans are intermediate chemicals, readily obtained from biomass, that can be converted to valuable fuels and chemicals. In particular, 5-hydroxymethylfurfural (HMF) can be derived from fructose through Brønsted acid catalyzed dehydration. HMF can, in turn, be converted to useful chemicals such as alkanes,[1] alkylated furans, for example, dimethylfuran (DMF),[2−4] and eventually to para-xylene.[5−10] HMF is therefore an important intermediate of the low temperature liquid phase catalytic production of valuable chemicals from biomass. Unfortunately, several side reactions also occur in the same acidic medium used to produce HMF from sugars: fructose and HMF can degrade to humins and HMF can rehydrate to formic acid (FA) and levulinic acid (LA). These unwanted reactions have been identified as the main obstacle to the profitable production of chemicals from HMF because of the loss of valuable sugars.[11] A clear understanding of the chemistry is lacking, despite the heightened effort to improve HMF production. An accurate understanding of the relationship between process parameters and reactivity is especially important when considering integrated temperature-sensitive separation processes, such as reactive adsorption.[12]

Several studies have analyzed kinetic data of hexose dehydration or HMF rehydration at varying temperatures or pH values.[13−19] Patil and Lund considered the rate of HMF degradation to FA, LA, and humins at different acid concentrations and temperatures.[13] They concluded that HMF degradation is linearly dependent on acid concentration, in agreement with an earlier study by Kuster and Temmik.[14] However, Patil and Lund's work did not consider fructose degradation in addition to that of HMF. Girisuta et al. have studied the kinetics of homogeneous catalyzed LA formation, between 140 and 200 °C, using either glucose[15] or HMF[16] as starting materials. They fitted their data considering the effects

Received: October 20, 2013
Revised: December 4, 2013
Published: December 6, 2013

of both catalyst concentration and temperature assuming a power-law dependence of the reaction rates on catalyst and substrate concentrations. All of the fitted power law constants fell between 0.88 and 1.38, close to the linear relationships found in other work. Baugh and McCarty have also considered glucose decomposition to HMF and LA at 170−230 °C.[17] They concluded that base catalysis accounts for monosaccharide decomposition at pH > 2.5, though this may be a case of over fitting, as the concentration of hydroxide ions is still very low at those pH values. Asghari and Yoshida studied the kinetics of acid-catalyzed fructose dehydration between 210 and 270 °C.[18] They considered a range of pH values, though they did not quantify the effect of acid concentration, rather they relied on heuristic approaches to select an optimum pH. Their reaction network included several reactions not present in other studies, such as fructose degradation to furfural and degradation reactions of FA and LA. These reactions may be important at the higher temperatures of their study, but are not observed as much at lower temperatures (<200 °C). Finally, Kuster and van der Steen studied the dehydration of fructose in a stirred tank reactor at temperatures of 170−213 °C using phosphoric acid catalyst.[19] As they focused primarily on reactor design, they did not consider each reaction individually, but rather lumped fructose conversion to HMF and humins as well as HMF degradation to FA/LA and humins. The data analysis in these experimental papers requires rate laws, which are usually determined using a heuristic approach. The approach taken to define the rate laws can be improved through better integration with fundamental studies.

In addition to the phenomenological approaches described above, several mechanisms for fructose dehydration have been proposed based on first principles computational methods.[20−23] Unfortunately, there is little agreement on many of the intermediate steps. Assary et al. used high-level theory to show that protonated fructose reacts much more readily than the neutral form and that the mechanism proceeds through a closed-chain pathway.[20] This agrees with experimental observations that the rate of fructose dehydration to HMF depends on pH.[17] Caratzoulas and Vlachos proposed a nine step reaction pathway based on Quantum Mechanics/Molecular Mechanics (QM/MM) simulations with explicit water, concluding that an intramolecular hydride transfer is the rate-controlling step in the reaction.[21] Their QM/MM approach includes the solvent explicitly, showing that water can actively participate in the reaction by facilitating proton transport. Consequently, only a single first-principles-based microkinetic modeling study has been published so far.[22] Development of detailed models has been challenging because gas-phase or implicit solvent calculations fail to quantitatively account for solvent effects.

Fructose may react in solution through many different simultaneous reactions. The computational expense of accurately estimating the activation energy of each elementary step makes examination of multiple reaction pathways for each reaction a difficult and time-consuming task. Yang et al. calculated the thermochemistry, a less computationally intensive approach, of a large number of reaction paths.[23] While these paths give information about a wide range of possible reactions, accurate modeling of the reaction kinetics is not possible without information about the transition states. As a result, microkinetic modeling of the different reaction paths is impossible with the currently available knowledge. Moreover, performing theoretical calculations when the molecular structure of products is not known, as in the case of humins, remains a challenge. While recent work by Patil et al. used IR spectroscopy and found that humin structure is consistent with aldol condensation chemistry initiated by a reactive HMF degradation product,[13,24] it is not yet known if the HMF degradation product is the only initiator for humin formation. Indeed, a recent paper by van Zandvoort et al. concluded that other chemistries, including dehydration, are important as well.[25] Currently, a purely theoretical model for the entire reaction network is not possible, because of the prevalence of parallel reactions and unknown products. An approach that balances theoretical fidelity with practicality is therefore necessary to gain insights into the whole system.

The aim of the present work is to develop an understanding of fructose dehydration and HMF rehydration kinetics and develop a skeleton model that captures most of the essential physics, while being minimalistic, and integrates experimental and computational insights. This model accounts for the first time for (1) the tautomeric distribution of fructose, (2) the increased fraction of formic acid compared to levulinic acid when starting from fructose,[26] and (3) the correct rate-limiting step as revealed by first-principles computational studies[22] and kinetic isotope experiments. The model describes a new, comprehensive kinetics data set at low and intermediate temperatures and various pH values presented herein. These relatively low temperatures are relevant because we envision a process that couples glucose-to-fructose isomerization using Lewis acids, which is favorable at these temperatures,[27,28] with fructose dehydration to HMF. A plug flow reactor model based on these kinetics is used to indicate optimal operating conditions. The model indicates that operating at these temperatures has certain advantages from a practical standpoint. The theoretical and experimental justification for the modular form of the model used in the present work is addressed before presenting and discussing the experimental results.

EXPERIMENTAL AND COMPUTATIONAL METHODS

Materials. Fructose 99% (Sigma Aldrich), 5-(Hydroxymethyl)furfural (HMF) 98% (Sigma Aldrich), levulinic acid (LA) 98% (Sigma Aldrich liquid form), formic acid (FA) 88% (Fisher Scientific), hydrochloric acid, (HCl), 1 M (Sigma Aldrich), potassium chloride, (KCl), 98% (Merck), and distilled water were used for solution preparation. Deuterated fructose (1-D, 97%) was purchased from Cambridge Isotope Laboratories, Inc. and was used without any further treatment.

Reaction Kinetics. Experiments with different initial compositions of fructose, HMF, and LA were carried out in buffer solutions of pH = 0.7, 1.1, and 1.6, as well as in water (for fructose only). These solutions were prepared by mixing appropriate quantities of HCl and KCl (for details see Supporting Information). The buffer solution was added to a 100 mL volumetric flask containing the appropriate amounts of the reactants. Thirteen 5 mL glass reactors with an internal conical bottom and a conical magnetic stirring bar were preheated in an aluminum heating block filled with silicon oil. An aliquot portion of the reaction solution was added to each of the preheated glass reactors through the septum of the top cover. The temperature was monitored with an external thermometer and a thermocouple inserted into each sealed reactor. The time at which the test solution was added to the

dx.doi.org/10.1021/cs4009495 | ACS Catal. 2014, 4, 259−267

glass reactor was considered as the starting point for data collection. Reactor vials were removed at regular time intervals and immediately quenched in an ice-bath before collecting a sample for analysis.

An accounting of all reaction temperatures and pH values is shown in Table 1. The temperature variation during each experiment was ±2−3 °C. Overall, we have conducted 45 different kinetic experiments starting with varying concentrations of either fructose or HMF comprising over 1500 data points in total. Temperatures between 74 and 147 °C and pH values of 0.7, 1.1, and 1.6 are studied.

Table 1. Experimental Conditions for Kinetics Experiments in Aqueous Solution[a]

pH	starting materials	temperature, °C
0.7	10%w/v fructose	74, 100, 114, 124, and 147
	5%w/v HMF	74, 100, 114, 124, and 147
1.1	10%w/v fructose	74, 84, 86, 95, 104, 109, 112, 120, 126, and 138
	5%w/v HMF	74, 88, 89, 99, 109, 110, 114, 121, 130, and 141
	10%w/v fructose + 5%w/v HMF	111
	20%w/v fructose	111
	5%w/v fructose	111
	10%w/v HMF	111
	2.5%w/v HMF	111
1.6	10%w/v fructose	74, 99, 109, 118, and 143
	5%w/v HMF	74, 104, 111, 121, and 143

[a]HCl is used as a catalyst. A total of 45 experiments were conducted.

Analytical Methods. Samples from the reactors were further diluted in 1 to 10 ratio with distilled water and analyzed with HPLC (2695 Waters) using an Aminex HPX-87H ion exchange column and a Refractive Index detector (RI 2414). A 5 mM solution of sulfuric acid was used as mobile phase with a flow rate 0.65 mL/min. The temperature of the column oven was 65 °C, and the temperature of the RI was 35 °C. Calibration curves were built of all the known compounds and used for the quantification of reactants and products.

Computational Methods. Experimental data were processed simultaneously using the *lsqnonlin* nonlinear fitting function of Matlab, which utilizes a trust-region-reflexive algorithm to perform local minimization. The quality of fit to each component was determined using the normalized root-mean-square error (NRMSE) (see Supporting Information). Each experiment starting from fructose produced a concentration profile similar to that shown in Figure 1. As fructose degrades, HMF is the majority product at short times. After around 75 min, the HMF concentration reaches a maximum as the rate of HMF production from fructose equals the rate of HMF degradation to levulinic acid (LA), formic acid (FA), and humins. At longer times, FA and LA become the dominant products, as they do not degrade appreciably under these conditions. A batch reactor model was used to describe the experimental data (see below).

To assess optimal conditions for continuous flow processing, species continuity equations are combined in an ideal plug flow reactor (PFR) model. The governing equation for the reactor is given in eq 1, where α_{ij} is either 1, −1, or 0 depending on if component i is a product, reactant, or does not participate (respectively) in reaction j; and τ is the space time of the reactor, defined as the reactor volume V divided by the inlet volumetric flow rate F. Equation 1 is evaluated analytically for fructose and HMF concentrations.

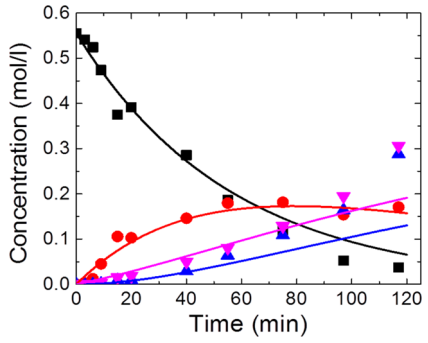

Figure 1. Characteristic concentration profile of fructose (black squares), HMF (red circles), LA (blue triangles), and FA (magenta triangles) with model predictions (lines) for comparison. Reaction carried out with 10%w/v fructose in an aqueous HCl-KCl buffer (pH = 1.1) at T = 120 °C.

$$\tau = \int_{C_i^0}^{C_i} \frac{dC_i}{\sum_j \alpha_{ij} R_j} \quad (1)$$

REACTION NETWORK DEVELOPMENT

Tautomer Equilibrium. Fructose has five different tautomeric forms in equilibrium in solution, as shown in Scheme 1. There are two furanose tautomers (α- and β-furanose), two pyranose tautomers (α- and β-pyranose), and one open chain tautomer. Bicker et al. proposed that the relative abundance of fructo-furanose in nonaqueous solvents explains the selectivity to HMF in those solvents based on the structural similarities between fructo-furanose and HMF.[29,30] Moreover, Amarasekara et al. propose that both α- and β-furanose are active for dehydration in DMSO.[31] A recent paper from Dumesic's group supports this conclusion for solvent mixtures of water and tetrahydrofuran.[32] Akien et al. concluded that fructo-pyranose can only lead to HMF through the formation of fructose anhydrides based on an NMR study;[33] the formation of these anhydrous compounds is generally unfavorable in water. On the basis of previous work, we consider that fructose dehydrates to HMF from its furanose form and that the pyranose and open chain forms equilibrate

Scheme 1. Tautomeric Forms of Fructose in Solution

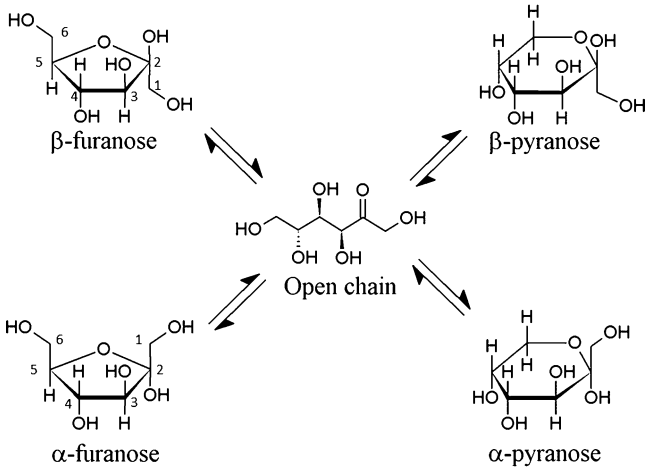

dx.doi.org/10.1021/cs4009495 | ACS Catal. 2014, 4, 259−267

sufficiently fast, compared to the dehydration and rehydration kinetics, to replenish the furanose form.

Kimura et al. have measured the concentrations of all tautomers in solution at different temperatures using ^{13}C NMR.[34] Their data are in general agreement with those reported by other groups.[35,36] We fitted their data to the van't Hoff equation (eq 2) to estimate parameters needed to describe the equilibrium at temperatures between 30 and 150 °C. These parameters are shown in Table 2 and the fits in Figure 2. The

Table 2. Parameters of Fructose Tautomer Equilibria Fitted on Data by Kimura et al.[34]

tautomer ratio	$ij = \beta\ p$	$ij = \beta\ f$	$ij = \alpha\ p$	$ij = \alpha\ f$
K_{ij} (T = 303 K)	59.2	26.4	0.6	6.4
ΔH_{ij}, kJ/mol	−30.2	−19.0	−5.5	−14.2

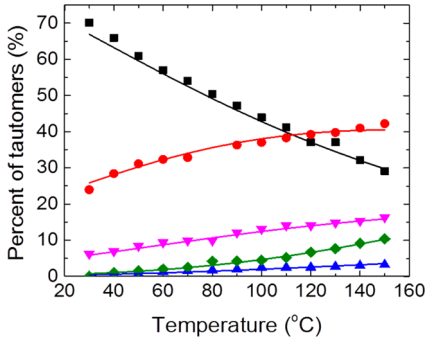

Figure 2. Fitted tautomer distribution of fructose in water (lines), based on ^{13}C NMR by Kimura (symbols).[34] α-Pyranose (blue triangles), β-pyranose (black squares), α-furanose (magenta triangles), β-furanose (red circles), and open-chain (green diamonds).

furanose fraction at each temperature is related to the corresponding equilibrium constants via eq 3:

$$K_{ij}(T) = \frac{C_{ij}^{\mathrm{Fru}}}{C_{\mathrm{OC}}^{\mathrm{Fru}}} = K_{ij}(T = 303\ \mathrm{K}) \cdot \exp\left[\frac{-\Delta H_{ij}}{R}\left(\frac{1}{T} - \frac{1}{303\ \mathrm{K}}\right)\right] \quad (2)$$

$$\phi_f = \frac{K_{\alpha f}(T) + K_{\beta f}(T)}{1 + K_{\alpha f}(T) + K_{\beta f}(T) + K_{\alpha p}(T) + K_{\beta p}(T)} \quad (3)$$

Here, K_{ij} is the equilibrium constant for the conversion of fructose in the open chain form to the ij form, with $i = \alpha, \beta$ for α or β forms of furanose and pyranose configurations ($j = f, p$), T is the temperature in Kelvin, ΔH_{ij} is the (fitted) enthalpy difference between the tautomers, R is the gas constant, ϕ_f is the fraction of fructose in the furanose form (either α or β forms). The change in the distribution of tautomers with temperature is included below in our skeleton model of fructose dehydration. Importantly, this framework can easily be extended to account for the effect of mixed solvents (not addressed herein) on the relative concentrations and thus on rate of dehydration.

Fructose Dehydration Skeleton Model. Prior quantum mechanics/molecular mechanics (QM/MM) molecular dynamics (MD) simulation by Caratzoulas and Vlachos suggested that there are two key elementary steps in the dehydration of fructose to HMF: a hydride transfer from C1 to C2 and a hydride transfer from C5 to C4 (for carbon atom numbering see Scheme 1).[21] Further microkinetic modeling by Nikbin et al. using the first-principles QM/MM free energies of ref 21 and an adjustable parameter suggested that while the activation energy of the C5−C4 hydride transfer is higher, the C1−C2 hydride transfer is actually rate-limiting.[22]

To assess the model prediction for the rate limiting step, we carried out isotopic-labeling experiments. Kinetics experiments starting with labeled fructose (deuterated at C1) were performed and compared with the normal fructose case. If hydrogen transfer from C1 to C2 is the rate limiting step, then replacing hydrogen with deuterium at C1 of fructose could slow down the fructose disappearance rate, known as kinetic isotope effect (KIE).[37] Figure 3 shows the time progression of fructose conversion and HMF yield. The fructose disappearance rate is significantly slower for fructose-1-D compared to the normal fructose case indicating the presence of prominent KIE (Figure 3a). A similar trend is observed in the HMF yield (Figure 3b). This trend has held up in repeated experiments. These results confirm that the hydrogen transfer from C1 to C2 is the rate-limiting step in fructose conversion to HMF under these conditions.

We conclude that the fructose dehydration can be reduced to the overall two-step reaction shown in Scheme 2. The first step contains the elementary reactions that occur before the hydride transfer, while the second step constitutes the hydride transfer itself. It is assumed that all downstream reactions do not affect the overall rate of reaction. Even though Yang et al.[23] and Assary et al.[38] postulate different dehydration mechanisms than Caratzoulas and Vlachos,[21] all studies agree that the reaction

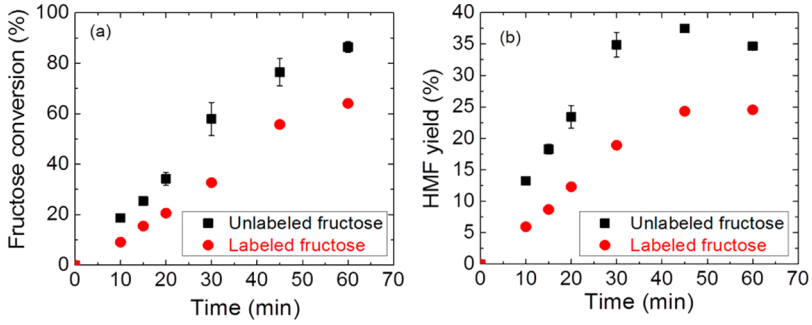

Figure 3. Fructose conversion (a) and HMF yield (b) as a function of time with normal fructose and labeled fructose at the C1 position (fructose-1-D). Reactions were carried out with an initial concentration of 1%w/v fructose dissolved in 0.1 M aqueous HCl solution, and the oil bath was maintained at 140 °C in water.

dx.doi.org/10.1021/cs4009495 | ACS Catal. 2014, 4, 259−267

Scheme 2. Reduced Two-Step Fructose Dehydration Reaction Scheme[a]

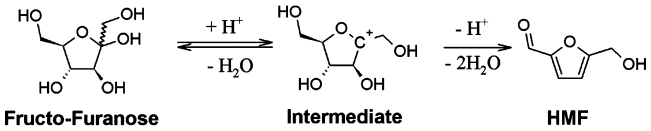

[a]The first step describes the reversible proton attachment/dehydration step. The rate of the second step describes the intrahydride transfer from C1 to C2. Subsequent elementary steps following the intrahydride transfer are considered to be fast and irreversible under our conditions.

proceeds with an initial protonation and dehydration of the OH on C2 which eventually forms the same intermediate considered in this work. Consequently, the skeleton model developed in this work, which was developed based on the work of Caratzoulas and Vlachos,[21] captures the initial chemistry of all three reaction mechanisms. It is important to note that the hydride transfer does not explicitly involve a Brønsted acid and as a result, the rate of the elementary step does not depend on proton concentration. This appears to contradict the experimental finding that the measured reaction rate is first-order in proton concentration. We reconcile this apparent paradox below by recognizing that the measured reaction rate depends on the concentration of the intermediate in the hydride transfer that in turn has proton dependence.

The informed decision to treat the first dehydration product as the reactive intermediate allows us to explicitly consider two independent reactions: fructose dehydration to the intermediate (equilibrium limited) and intermediate reaction to HMF (irreversible, kinetically controlled). The equilibrium constant is estimated using thermodynamic information from the previous QM/MM model[22] in eq 4, where ΔU = 105 kJ/mol and ΔS = 271 J/mol/K. The concentration of water, which participates in the equilibrium and therefore should be included, is estimated using the DIPPR database.[39]

$$K_{DH}(T) \approx \frac{C_{Int}C_{H_2O}}{C_{Fru}C_{H+}} = \exp\left[\frac{-(\Delta U - T\Delta S)}{RT}\right] \quad (4)$$

Even though the hydride transfer is not acid catalyzed, the concentration of the intermediate directly preceding the hydride transfer is proportional to the proton concentration. This can explain the experimentally observed first-order dependence of dehydration rate on C_{H+} (see also eq 5).

Excess Formic Acid Formation. The stoichiometry of HMF rehydration indicates that FA and LA should form equimolarly, that is, FA and LA should also form in equal molar ratios if both are produced solely via HMF rehydration. Figure 4 shows the ratio of FA to LA as a function of fructose or HMF conversion for all of our experiments. The FA:LA ratio is close to 1 when HMF is the initial reactant, but more FA forms than LA when fructose is the reactant. This observation is consistent across different reactant conditions.

A plausible source for the excess FA can be deduced by careful consideration of experimental data. Without considering the chemical feasibility of the following reactions, the excess FA can be attributed to LA reacting with fructose, HMF, itself, or humins; either HMF or fructose producing more FA than LA through an as-yet unknown pathway; LA fragmenting to form FA or other products; or LA selectively adsorbing on humins.

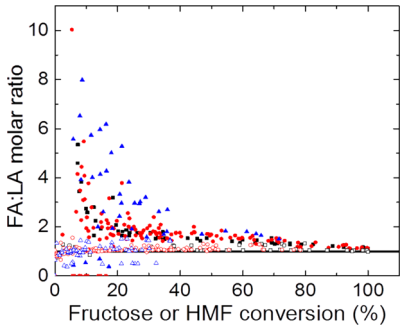

Figure 4. Ratio of FA:LA as a function of conversion of fructose (filled symbols) or HMF (open symbols) at every experimental time point with different symbols corresponding to pH = 0.7 (black squares), 1.1 (red circles), and 1.6 (blue triangles). Unity (horizontal line) highlighted for reference. HMF hydration results in nearly equimolar FA/LA mixtures. In contrast, fructose dehydration results in excess FA compared to LA indicating a direct pathway to FA formation that does not involve HMF as an intermediate.

However, the highest ratio of FA:LA occurs at low conversions, where humin formation is minimal, so LA adsorption should be negligible. LA solutions have been shown to be unreactive under the conditions of our experiments (Supporting Information), ruling out the possibility of LA fragmenting to FA or being removed from solution via LA-LA condensation. When HMF is used as a reactant, no excess FA is observed, so it can be concluded that there is neither reaction of LA with HMF, adsorption on humins, nor HMF degradation to form more FA than LA, as these reactions would occur when starting from both fructose and HMF. This leaves two possibilities: LA may react with fructose or a fructose-derived intermediate, leaving behind excess FA, or fructose may produce FA directly. Since the FA:LA ratio decreases with conversion (Figure 4), the pathway that produces FA from fructose must be prevalent at the beginning of the reaction, that is, fructose must directly produce FA rather than reacting with the LA that is produced from HMF. This reaction should form other products as well. Two unidentified products in HPLC analysis formed at the same reaction time as excess FA, though this may be coincidental. They degraded quickly, suggesting they could initiate or participate in humin formation. Attempts to identify these compounds by comparing HPLC retention times to standard solutions were unsuccessful; many compounds were ruled out, including pyruvaldehyde, lactic acid, glyceraldehyde, dihydroxyacetone, and furfural. Other kinetic studies do not appear to have treated this reaction explicitly. However, Yang et al. examined the thermochemistry of several different reaction pathways of β-fructo-furanose.[23] While the text of the article focuses on one particular pathway, the Supporting Information contains a total of 24 pathways. Of these, one produces FA without leading to LA or HMF, suggesting that such a reaction might be plausible.

Reaction Orders. The assumption that fructose dehydration proceeds with a first-order dependence on catalyst and reactant has been used in some of the literature.[13,40,41] However, Girisuta et al. have used power-law relations to describe the kinetics, concluding that the exponents are close to unity.[15,16,42] To avoid adding unnecessary parameters, a linear dependence on catalyst and reactant is assumed in the present work unless this assumption can be shown to be inadequate.

For first-order kinetics, the conversion should be independent of the initial concentration of the substrate. Figure 5 shows

dx.doi.org/10.1021/cs4009495 | ACS Catal. 2014, 4, 259−267

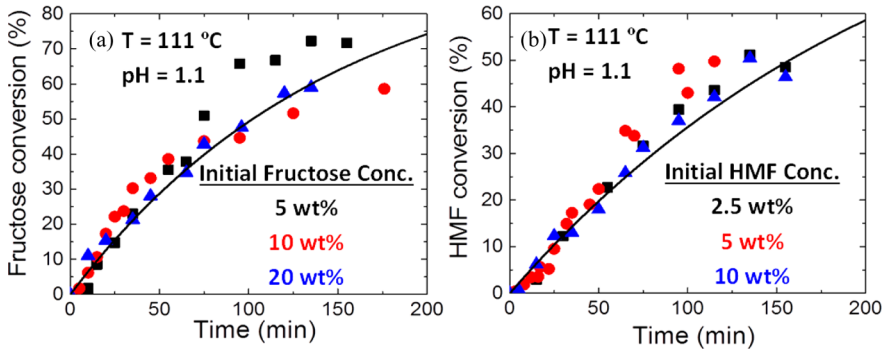

Figure 5. Conversion of fructose (a) and HMF (b) as a function of time starting from different initial concentrations. Black line indicates model prediction. The model assumes there is no effect of initial concentration on conversion rate, so only one line is shown.

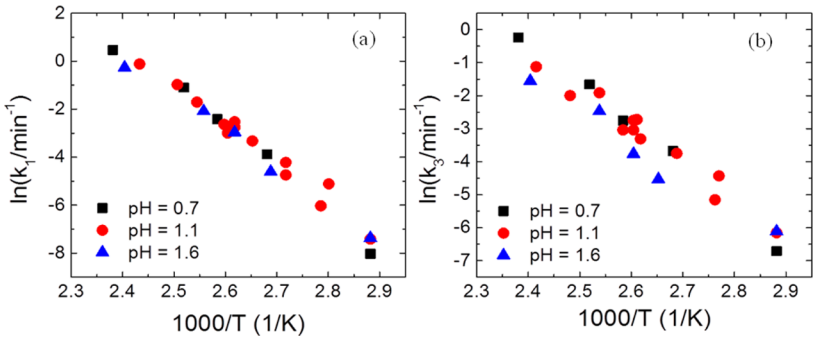

Figure 6. Reaction rate constants for fructose dehydration to HMF (a) and HMF rehydration to formic and levulinic acids (b) at various values of pH. The collapse of the data in each case indicates that the intrinsic rate constants are, within experimental error, independent of pH, and the reaction rates are first-order on proton concentration.

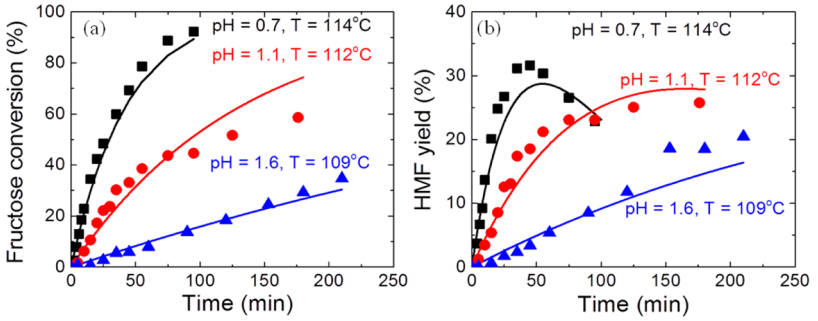

Figure 7. Comparison between model (line) and experimental data (symbols) for fructose conversion (a) and HMF yield (b) at different pH values.

that the conversion of both fructose and HMF are independent of substrate concentration, supporting the conclusion that the reaction is first-order in each substrate. Similarly, if the reactions are treated as essentially first-order with respect to catalyst concentration, the fitted rate constants of the individual experiments should be independent of catalyst concentration. The Arrhenius plots in Figure 6 show that the rate constants for fructose dehydration and HMF rehydration are essentially independent of pH when a first-order dependence on proton concentration is already included explicitly. The same reaction orders apply to other reactions, including humin formation whose exact pathway is unknown (Supporting Information). Furthermore, Figure 7 shows that the model can accurately describe fructose conversion and HMF yield at T = 112 °C as pH changes. Another example of model performance is also shown in Figure 1. A parity plot, given in the Supporting Information, shows that the model satisfactorily describes the concentrations of each component.

Functional Form of the Model. Scheme 3 shows the reaction network that includes three important elements that were discussed above: (1) the fructose tautomerization, (2) the two-step lumped model of fructose dehydration guided from the microkinetic model based on QM/MM simulations and KIE experiments, and (3) a direct pathway from fructose to FA.

Scheme 3. Proposed Mechanism for Acid-Catalyzed Reactions of Fructose and HMF in Aqueous Solution

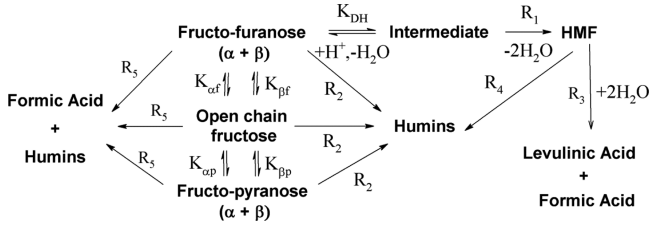

dx.doi.org/10.1021/cs4009495 | ACS Catal. 2014, 4, 259−267

In addition, it accounts for side reactions to humins. The resulting reaction network contains five reactions R1−R5 acting on four directly measurable species (fructose, HMF, FA, and LA) with six implicit species (five fructose tautomers and a reactive intermediate). The measurable species balances are given in eq 5 in terms of reaction rates given by eqs 6−10. The implicit species, in particular fructo-furanose and the reactive intermediate, are accounted for through the equilibrium relations in eqs 2−4. Equation 5 represents a series of ordinary differential equations for a batch reactor.

$$\frac{dC_i}{dt} = \sum_{j=1}^{5} \alpha_{ij} R_j \tag{5}$$

$$R_1 = k_1 \phi_f C_{Fru} \left(\frac{K_{DH} C_{H^+}}{C_{H_2O}} \right) \tag{6}$$

$$R_2 = k_2 C_{Fru} C_{H+} \tag{7}$$

$$R_3 = k_3 C_{HMF} C_{H+} \tag{8}$$

$$R_4 = k_4 C_{HMF} C_{H+} \tag{9}$$

$$R_5 = k_5 C_{Fru} C_{H+} \tag{10}$$

Here, R_i is the rate of reaction i, C_i is the measurable concentration of component i, and α_{ij} is the same as eq 1. We assume that all forms of sugars undergo humin formation and the direct degradation to formic acid with the same rate. While this assumption is likely an oversimplification, there is very little literature data available on side reactions from nonfuranose forms of fructose, with most computational studies focusing on the β-furanose form.[23,38] Even though in a different solvent, Akien at al. proposed that both furanose and pyranose forms can degrade in DMSO,[33] and Assary and Curtiss suggested that open-chain fructose can also degrade in water.[43] Together, this limited number of studies supports the assumption that all forms of fructose can degrade.

PARAMETER ESTIMATION

Each rate constant is fit using two parameters to minimize numerical sources of error: the activation energy (p_1) and the logarithm of the rate constant at the temperature mean of all experiments (p_2). The fitted parameters are shown in Table 3

Table 3. Fitted Parameters p_1 and p_2 with Corresponding Pre-Exponential[a]

reaction[b]	$p_1 = E_a$, kJ/mol	$p_2 = \ln [k\ (T = 381K)/\text{min}]$	$\log_{10}[A_0/\text{min}]$
1	126 ± 2	1.42 ± 0.05	17.9 ± 0.3
2	135 ± 8	−4.13 ± 0.16	16.7 ± 1.1
3	97 ± 1	−3.25 ± 0.02	11.9 ± 0.2
4	62 ± 9	−5.16 ± 0.24	6.2 ± 1.3
5	130 ± 10	−4.81 ± 0.19	15.7 ± 1.5

[a]Error margins correspond to 95% confidence interval. [b]See Scheme 3 for reaction numbers.

along with the familiar Arrhenius pre-exponential, derived from the corresponding fitted parameters. As prior literature has not considered fructose tautomerization, direct conversion of fructose to FA, and a two-step dehydration reaction, some parameters are expected to deviate slightly from previous reported values. Still, prior models include the same general reactions as the present work, that is, fructose dehydration, HMF rehydration, and humin production from fructose and HMF, so some comparison is possible. The fitted activation energy corresponds to the difference in energy between the intermediate and the transition state of the rate-limiting step. The apparent activation energy values reported in the literature assumed dehydration occurs in a single step. To compare these two values we need to combine the equilibrium constant in eq 4 with the rate constant in eq 6. Because of the entropic difference between fructose and the reactive intermediate, splitting the first-order reaction into a two-step mechanism results in an apparent activation energy of fructose dehydration that varies slightly depending on temperature: at 75 °C the apparent activation energy is 115 kJ/mol, while at 150 °C the apparent activation energy is 136 kJ/mol. A model that does not use a two-step model would report an apparent activation energy within that range in the same temperature span.

The activation energy for fructose dehydration reactions reported in Table 3 is consistent with the findings of Kuster and van der Steen.[19] They assumed fructose reacted to both HMF and humins via the formation of a common intermediate and measured an activation energy for the reaction of fructose to this intermediate as 130 kJ/mol.[19] As Table 3 shows, the activation energies of fructose dehydration to HMF, fructose conversion to humins, and fructose degradation to FA all fall near this value. Indeed, the similarity between each of these activation energies suggests that the reactions might undergo a similar rate-limiting elementary step, though validation of this conclusion is beyond the scope of the present work. Asghari and Yoshida's work at higher temperatures (T > 210 °C) has different activation energies for fructose degradation than those measured here.[18] They report an activation energy for fructose dehydration to HMF of 160 kJ/mol and an activation energy of the fructose degradation to humins of 101 kJ/mol. Their fructose dehydration activation energy is in line with the expected apparent activation energy when extrapolating our model to higher temperatures (152 kJ/mol).

The activation energies of HMF rehydration to FA and LA is in line with prior literature, but the measured activation energy of HMF degradation to humins differs somewhat from previous work. The energy for HMF rehydration reported here, 97 kJ/mol, is similar to that in other reports, which range from 89 to 111 kJ/mol.[13,16,18,19,40] However, the activation energy for HMF degradation to humins (62 kJ/mol) is lower than some reported values, which range from 94 to 115 kJ/mol,[13,16,19] but in line with that of Baugh and McCarty (56 kJ/mol).[17] The reason for the low activation energy is unclear. A better understanding of the HMF to humin reaction pathway is needed to properly quantify the reaction properties at low temperature.

Fructose tautomerization has an observable effect on the fitted rate constant for fructose dehydration. A kinetic model that does not account for the tautomeric distribution of fructose would report a lower rate constant for the fructose to HMF reaction. Figure 8 shows this effect, as the apparent rate of fructose dehydration is underestimated by nearly a factor of 2 when tautomers are not included. The difference between the rate constants changes slightly with temperature (factors of 2.25 at 90 °C and 1.8 at 130 °C) and can be related to the change in tautomer distribution in Figure 2. The effect of considering the tautomers on the reaction rate constant is more pronounced at low temperatures because the fraction of furanosic fructose is higher at high temperatures.

dx.doi.org/10.1021/cs4009495 | ACS Catal. 2014, 4, 259−267

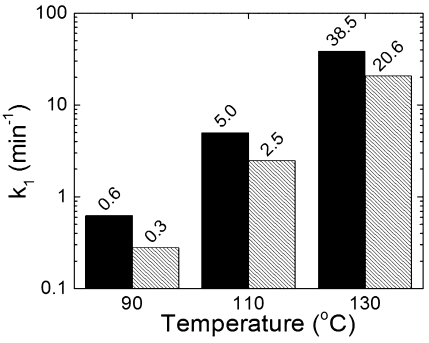

Figure 8. Fitted rate constant for fructose dehydration at three temperatures when tautomer distribution is included (solid) and not explicitly included (hashed). Neglecting tautomer distribution leads to under-estimating the rate constant of fructose dehydration by a factor of 2.

The normalized root-mean-square error (NRMSE) for each component is given in Table 4. Fructose and HMF are well-described by the present model. However, the description of FA and LA is only fair. One possible explanation is that fructose and HMF are fit at the expense of FA and LA. The concentrations of fructose and HMF are necessarily higher than those of the acids. The error minimization weighs the absolute magnitude of each error, so higher concentrations are fit more closely than low concentrations, relative to their magnitude. For example, if the experimental concentrations of HMF and LA are 0.2 and 0.05 M, respectively, fitted values of 0.18 and 0.04 M return a lower error than 0.16 and 0.045 M even though the percentage deviations (20% and 10%) are the same in each case. Regardless, the concentrations of fructose and HMF, which are the most important species, are captured adequately.

Table 4. NRMSE for Each Component

component	NRMSE
fructose	85.3%
HMF	84.0%
LA	69.5%
FA	71.7%

INSIGHTS INTO CONTINUOUS FLOW REACTOR DESIGN

The selectivity and yield of HMF in a reactor are examined next. Equation 1 was used to model the performance of the reactor as a function of the space time. Figure 9 shows fructose conversion and HMF yield at four different temperatures, with pH set to 0.7. The maximum achievable yield of HMF increases with increasing temperature because the HMF degradation reactions have lower activation energies than the fructose dehydration reaction. This finding is in line with the findings of prior studies.[30,40] When selectivity to HMF is plotted against fructose conversion (Figure 10), higher temperatures are found to have a higher selectivity for HMF for higher conversions. At low conversions, the selectivity does not vary much with temperature, as expected given the similarity in activation energies of fructose dehydration and degradation. A low conversion reactor, combined with separation and recycle, may be economically desirable. Caution should be used when the present model is extrapolated to higher temperatures, as other reactions not described by the model may then become significant. While optimizing the reactor design is beyond the scope of the present study, these insights could prove useful in further studies on the production of HMF from fructose.

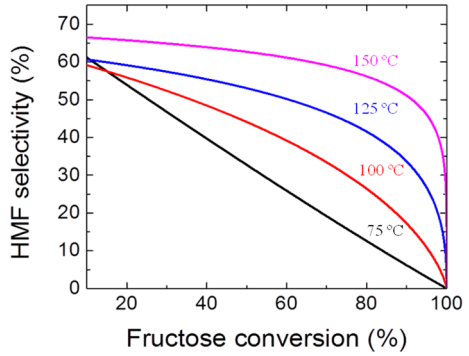

Figure 10. HMF selectivity as a function of fructose conversion in a PFR at different temperatures and buffered pH = 0.7. A temperature of 150 °C gives higher HMF selectivities and yields than lower temperatures.

CONCLUSIONS

Fructose dehydration and HMF rehydration kinetics in aqueous HCl were measured over a range of temperatures, pH, and

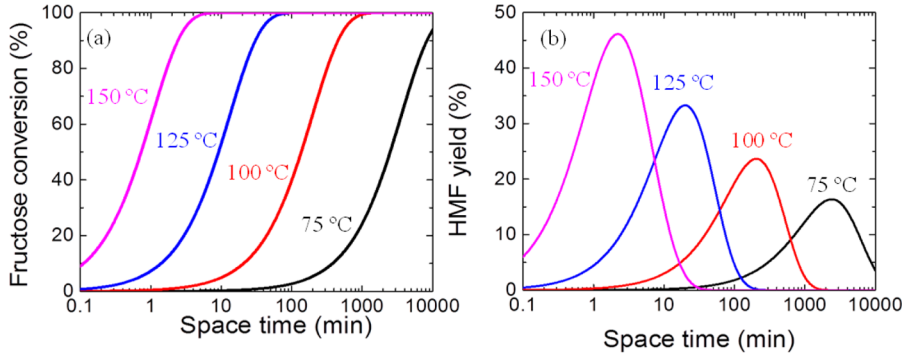

Figure 9. Fructose conversion (a) and HMF yield (b) as a function of space time in a PFR at different temperatures and buffered pH = 0.7. Higher temperatures increase reaction rate as well as maximum obtainable HMF yield.

dx.doi.org/10.1021/cs4009495 | ACS Catal. 2014, 4, 259−267

substrate concentrations. Insights from KIEs on labeled fructose were combined with previous first-principles simulations to develop a skeleton mechanism of fructose dehydration, where the reaction proceeds by a rapid equilibrated protonation and first dehydration followed by a rate-limiting intrahydride transfer. In addition, our model includes for the first time tautomerization and the experimentally observed molar excess of formic acid to levulinic acid.

It has been found that the tautomeric equilibrium of various forms of sugars plays an important role in the rate constants of fructose dehydration. The model described the concentration profiles of fructose and HMF well using first-order kinetics in substrate and proton concentration. The observed first-order dependence of the fructose dehydration rate on proton concentration despite the fact that the hydride transfer, which is the rate limiting step, does not explicitly involve a Brønsted acid, is explained by recognizing that the measured reaction rate depends on the concentration of the intermediate before the hydride transfer that is proportional to the proton concentration. A continuous flow reactor model based on the kinetics developed here identified HMF selectivity as much more sensitive to temperature effects when the reactor is operated at high fructose conversions. At low conversions (∼15%), HMF selectivity is less dependent on temperature.

■ ASSOCIATED CONTENT

Supporting Information

Buffer solution compositions, details of fitting procedure and parity, experimental evidence that levulinic acid does not react under our conditions, and evidence that all rates are proportional to acid concentration. This material is available free of charge via the Internet at http://pubs.acs.org.

■ AUTHOR INFORMATION

Corresponding Authors

*E-mail: vlad@udel.edu (V.N.).
*E-mail: vlachos@udel.edu (D.G.V.).

Notes

The authors declare no competing financial interest.

■ ACKNOWLEDGMENTS

This work was supported as part of the Catalysis Center for Energy Innovation, an Energy Frontier Research Center funded by the U.S. Department of Energy, Office of Science, and Office of Basic Energy Sciences under award number DESC0001004. The authors would also like to thank Dr. George Tsilomelekis and Professor Bingjun Xu for assisting with part of the KIE experiments as well as help with understanding the results.

■ REFERENCES

(1) Assary, R. S.; Redfern, P. C.; Hammond, J. R.; Greeley, J.; Curtiss, L. A. *Chem. Phys. Lett.* **2010**, *497*, 123.
(2) Thananatthanachon, T.; Rauchfuss, T. B. *Angew. Chem., Int. Ed.* **2010**, *49*, 6616.
(3) Kazi, F. K.; Patel, A. D.; Serrano-Ruiz, J. C.; Dumesic, J. A.; Anex, R. P. *Chem. Eng. J. (Lausanne)* **2011**, *169*, 329.
(4) Jae, J.; Zheng, W.; Lobo, R. F.; Vlachos, D. G. *ChemSusChem* **2013**, *6*, 1158.
(5) Williams, C. L.; Chang, C. C.; Do, P.; Nikbin, N.; Caratzoulas, S.; Vlachos, D. G.; Lobo, R. F.; Fan, W.; Dauenhauer, P. J. *ACS Catal.* **2012**, *2*, 935.
(6) Do, P. T. M.; McAtee, J. R.; Watson, D. A.; Lobo, R. F. *ACS Catal.* **2013**, *3*, 41.
(7) Cheng, Y. T.; Huber, G. W. *Green Chem.* **2012**, *14*, 3114.
(8) Wang, D.; Osmundsen, C. M.; Taarning, E.; Dumesic, J. A. *ChemCatChem* **2013**, *5*, 2044.
(9) Chang, C.-C.; Green, S. K.; Williams, C. L.; Dauenhauer, P. J.; Fan, W. *Green Chem.* **2013**, DOI: 10.1039/C3GC40740C .
(10) Lin, Z. J.; Ierapetritou, M.; Nikolakis, V. *AIChE J.* **2013**, *59*, 2079.
(11) Torres, A. I.; Daoutidis, P.; Tsapatsis, M. *Energ Environ Sci* **2010**, *3*, 1560.
(12) Swift, T. D.; Bagia, C.; Nikolakis, V.; Vlachos, D. G.; Peklaris, G.; Dornath, P.; Fan, W. *AIChE J.* **2013**, *59*, 3378.
(13) Patil, S. K. R.; Lund, C. R. F. *Energy Fuels* **2011**, *25*, 4745.
(14) Kuster, B. F. M.; Temmink, H. M. G. *Carbohydr. Res.* **1977**, *54*, 185.
(15) Girisuta, B.; Janssen, L. P. B. M.; Heeres, H. J. *Chem. Eng. Res. Des.* **2006**, *84*, 339.
(16) Girisuta, B.; Janssen, L. P. B. M.; Heeres, H. J. *Green Chem.* **2006**, *8*, 701.
(17) Baugh, K. D.; McCarty, P. L. *Biotechnol. Bioeng.* **1988**, *31*, 50.
(18) Asghari, F. S.; Yoshida, H. *Ind. Eng. Chem. Res.* **2007**, *46*, 7703.
(19) Kuster, B. F. M.; Van Steen, H. J. C. D. *Starch/Stärke* **1977**, *29*, 99.
(20) Assary, R. S.; Redfern, P. C.; Greeley, J.; Curtiss, L. A. *J. Phys. Chem. B* **2011**, *115*, 4341.
(21) Caratzoulas, S.; Vlachos, D. G. *Carbohydr. Res.* **2011**, *346*, 664.
(22) Nikbin, N.; Caratzoulas, S.; Vlachos, D. G. *ChemCatChem* **2012**, *4*, 504.
(23) Yang, G.; Pidko, E. A.; Hensen, E. J. M. *J. Catal.* **2012**, *295*, 122.
(24) Patil, S. K. R.; Heltzel, J.; Lund, C. R. F. *Energy Fuels* **2012**, *26*, 5281.
(25) Wyman, M. *Smithsonian* **2000**, *31*, 18.
(26) Kuster, B. F. M.; Tebbens, L. M. *Carbohydr. Res.* **1977**, *54*, 158.
(27) Moliner, M.; Román-Leshkov, Y.; Davis, M. E. *Proc. Natl. Acad. Sci. U.S.A.* **2010**, *107*, 6164.
(28) Choudhary, V.; Mushrif, S. H.; Ho, C.; Anderko, A.; Nikolakis, V.; Marinkovic, N. S.; Frenkel, A. I.; Sandler, S. I.; Vlachos, D. G. *J. Am. Chem. Soc.* **2013**, *135*, 3997.
(29) Bicker, M.; Hirth, J.; Vogel, H. *Green Chem.* **2003**, *5*, 280.
(30) Bicker, M.; Kaiser, D.; Ott, L.; Vogel, H. *J. Supercrit. Fluids* **2005**, *36*, 118.
(31) Amarasekara, A. S.; Williams, L. D.; Ebede, C. C. *Carbohydr. Res.* **2008**, *343*, 3021.
(32) Tucker, M. H.; Alamillo, R.; Crisci, A. J.; Gonzalez, G. M.; Scott, S. L.; Dumesic, J. A. *ACS Sustainable Chem. Eng.* **2013**, *1*, 554.
(33) Akien, G. R.; Qi, L.; Horvath, I. T. *Chem. Commun. (Cambridge, U. K.)* **2012**, *48*, 5850.
(34) Kimura, H.; Nakahara, M.; Matubayasi, N. *J. Phys. Chem. A* **2013**, *117*, 2102.
(35) Lichtenthaler, F. W.; Ronninger, S. *J. Chem. Soc., Perkin Trans. 2* **1990**, 1489.
(36) Barclay, T.; Ginic-Markovic, M.; Johnston, M. R.; Cooper, P.; Petrovsky, N. *Carbohydr. Res.* **2012**, *347*, 136.
(37) Westheimer, F. H. *Chem. Rev.* **1961**, *61*, 265.
(38) Assary, R. S.; Kim, T.; Low, J. J.; Greeley, J.; Curtiss, L. A. *Phys. Chem. Chem. Phys.* **2012**, *14*, 16603.
(39) Design Institute for Physical Properties, S. b. A.; Design Institute for Physical Property Research/AIChE.
(40) Weingarten, R.; Cho, J.; Xing, R.; Conner, W. C., Jr.; Huber, G. W. *ChemSusChem* **2012**, *5*, 1280.
(41) Kabyemela, B. M.; Adschiri, T.; Malaluan, R. M.; Arai, K. *Ind. Eng. Chem. Res.* **1999**, *38*, 2888.
(42) Girisuta, B.; Janssen, L. P. B. M.; Heeres, H. J. *Ind. Eng. Chem. Res.* **2007**, No. 46, 1696.
(43) Assary, R. S.; Curtiss, L. A. *Energy Fuels* **2012**, *26*, 1344.